Anisotropy of phonon modes in spontaneously ordered $GaInP_2$

M. J. Seong, A. Mascarenhas, and J. M. Olson
National Renewable Energy Laboratory, 1617 Cole Boulevard, Golden, Colorado 80401

Hyeonsik M. Cheong
Department of Physics, Sogang University, Seoul 121-742, Korea
(Received 14 November 2000; published 30 May 2001)

The anisotropy associated with angular variation of the phonon wave vector $\boldsymbol{q}$ with respect to the ordering axis $\boldsymbol{z}'$ of a spontaneously ordered $GaInP_2$ with order parameter $\eta \cong 0.46$ is studied by carefully performing micro-Raman measurements in scattering geometries where $\boldsymbol{q}$ is either parallel or perpendicular to $\boldsymbol{z}'$. The LO mode at $\sim 380\ cm^{-1}$ and the TO mode at $\sim 330\ cm^{-1}$ exhibit distinct phonon frequency shifts of $-1.2\ cm^{-1}$ and $+2.1\ cm^{-1}$, respectively, as the angle ϕ between $\boldsymbol{q}$ and $\boldsymbol{z}'$ varies from 0° to 90°. This small angular dispersion is explained on the basis of the bond-stiffening along the ordering axis with increasing order parameter η, providing strong evidence for a small A_1-E splitting in comparison to the large LO-TO splitting for these modes. In addition, an even larger angular dispersion, $+2.5\ cm^{-1}$, for the vibrational mode at $\sim 354\ cm^{-1}$ is observed. Two additional phonon modes, which have previously been labeled as *missing* to account for all nine Raman-active optical modes, are observed and experimentally identified with $E(x)$ and $E(y)$ tensors.

DOI: 10.1103/PhysRevB.63.235205 PACS number(s): 78.30.Fs, 63.20.Dj, 78.66.Fd

Spontaneous $CuPt_B$-type long-range ordering in $GaInP_2$ has been a subject of intense study in recent years.[1] Depending on the growth conditions, $Ga_{0.52}In_{0.48}P$ (written hereafter as $GaInP_2$ for simplicity), grown lattice-matched to a (001) GaAs substrate by organometallic vapor phase epitaxy (OMVPE), can exhibit ordering of the cations on the group-III sublattice along $[\bar{1}11]$ or $[1\bar{1}1]$, which are the two $[111]_B$ directions. The ordered alloys consist of monolayer superlattices of $Ga_{1+\eta}In_{1-\eta}P_2/Ga_{1-\eta}In_{1+\eta}P_2$ along the $[111]_B$ directions with the order parameter η ranging from 0 to 1. When the ordering is single variant, i.e., the ordering occurs along only one of the two $[111]_B$ directions throughout the sample, this structure has trigonal symmetry with point group C_{3v}, while the random alloy of $GaInP_2$ has the cubic zinc-blende structure with point group T_d.

The (001) backscattering Raman spectrum of the random alloy $GaInP_2$ consists of three major features:[2–10] a GaP-like longitudinal optical (LO) phonon peak at $\sim 380\ cm^{-1}$, an InP-like LO phonon peak at $\sim 362\ cm^{-1}$, and a transverse optical (TO) phonon band at $\sim 330\ cm^{-1}$. Since high-quality ordered $GaInP_2$ samples became available major effects of ordering on the (001) backscattering Raman spectrum have been reported:[7–10] three extra peaks at ~ 60, ~ 205, and $\sim 354\ cm^{-1}$ appear in the Raman spectra of highly ordered samples and the GaP-like LO phonon peak blue-shifts with increasing ordering by $\sim 1\ cm^{-1}$; The extra peaks are often interpreted in terms of the C_{3v} symmetry of the ordered alloy.[7–9] More recently, Cheong *et al.*[11] compared the results of micro-Raman scattering experiments in three different geometries with the phonon wave vector $\boldsymbol{q}$ either parallel or perpendicular to the ordering axis and obtained the first definitive phonon mode assignments for the extra Raman features originating from the spontaneous ordering effect.

Unlike crystals having the cubic zinc-blende structure with point group T_d, phonon modes in a uniaxial crystal exhibit anisotropy associated with the angular variation of the phonon wave vector $\boldsymbol{q}$ with respect to the uniaxis. Most experimental studies have focused on wurtzite-structure crystals with the C_{6v} point group symmetry.[12] Hence, spontaneously ordered $GaInP_2$ provides a unique opportunity to study the angular dispersion of polar-vibrational modes in uniaxial crystals with C_{3v} point group symmetry. In spite of its importance, however, the anisotropy associated with the angular variation of the phonon wave vector $\boldsymbol{q}$ with respect to the ordering axis has not received adequate experimental attention. At the zone center of the perfectly CuPt-ordered uniaxial crystal, a point group analysis yields nine Raman-active optical modes, i.e., $3A_1(z)+3E(x,y)$. One of the $E(x,y)$ modes has remained undiscovered until this work. In this paper, we report evidence of angular dispersions of the phonon modes at $\sim 330\ cm^{-1}$, $\sim 354\ cm^{-1}$, and $\sim 380\ cm^{-1}$, obtained by careful micro-Raman-scattering experiments in two different geometries with $\boldsymbol{q}$ either parallel or perpendicular to the ordering axis, and in addition, we report the discovery of the *missing* $E(x,y)$ mode.

We have performed micro-Raman measurements on several ordered $GaInP_2$ samples with order parameter $\eta \cong 0.46$, and the results for a typical sample presented in this paper were reproducible.[13] We choose the two cleavage directions of the samples as $X=[1\bar{1}0]$ and $Y=[110]$, and the growth direction as $Z=[001]$.[14] Since the sample is single variant, the principal axes of the crystal symmetry can be defined as the ordering axis $z'=[\bar{1}11]$ and two axes perpendicular to it: $y'=Y=[110]$ and $x'=[1\bar{1}2]$. The Raman spectra were measured, using the 7352-Å line from a tunable Ti:sapphire laser as the excitation source, in two geometries: backscattering on the (110) surface and right-angle scattering between the $\bar{Z}$ and $\bar{X}$ directions. In order to maintain consistency in the Raman shift of all spectra excited with the same incident photon energy and to minimize the spectral uncertainty, *the*

TABLE I. The C_{3v} Raman scattering efficiency calculated with Eqs. (1) and (2) for the scattering geometries employed in this work. We use Porto's notation where $\hat{k}_i(\hat{e}_i,\hat{e}_s)\hat{k}_s$ refers to the scattering configuration in which $\hat{k}_i$ and $\hat{k}_s$ are the propagation directions of the incident and scattered photons and $\hat{e}_i$ and $\hat{e}_s$ are the polarization directions of the incident and scattered photons, respectively. θ is the angle between the z' direction and the direction normal to the growth surface.

	A_1	$E_{x'}$	$E_{y'}$
$\overline{Z}(X,Z)\overline{X}$	$(a-b)^2\sin^2\theta\cos^2\theta$	$[c(\sin\theta\cos\theta)+d(\cos^2\theta-\sin^2\theta)]^2$	0
$\overline{Z}(Y,Y)\overline{X}$	a^2	c^2	0
$y'(z',z')\overline{y'}$	b^2	0	0
$y'(x',x')\overline{y}$	a^2	c^2	0
$y'(x',z')\overline{y'}$, $y'(z',x')\overline{y'}$	0	d^2	0

spectrometer was not moved throughout the entire set of measurements whose data were to be directly compared. Furthermore, we recorded the excitation laser line in all our Raman spectra to ensure that each spectrum was properly calibrated. It is important to emphasize that the uncertainty in the Raman shift of our spectrum is estimated to be $\sim 0.32\ \mathrm{cm}^{-1}$.[15]

In the C_{3v} symmetry, the three Raman scattering tensors A_1, $E_{x'}$, and $E_{y'}$ that represent vibrations along z', x', and y', respectively, can be written as[12]

$$\begin{pmatrix} a & 0 & 0 \\ 0 & a & 0 \\ 0 & 0 & b \end{pmatrix}, \quad \begin{pmatrix} c & 0 & d \\ 0 & -c & 0 \\ d & 0 & 0 \end{pmatrix}, \quad \begin{pmatrix} 0 & -c & 0 \\ -c & 0 & d \\ 0 & d & 0 \end{pmatrix}. \tag{1}$$

The Raman scattering efficiency can be written as

$$S \propto |\hat{e}_i \boldsymbol{R} \hat{e}_s|^2 \tag{2}$$

where $\hat{e}_i$ and $\hat{e}_s$ are the unit vectors along the polarizations of incident and scattered light, respectively, and $\boldsymbol{R}$ is the tensor for a particular mode. The values of $|\hat{e}_i \boldsymbol{R} \hat{e}_s|^2$ for the scattering geometries employed in this work are summarized in Table I.

In the backscattering geometry on the (110) cleaved surface, the phonon wave vector $\boldsymbol{q}$ is along the y' direction and perpendicular to the ordering axis; the $E_{y'}$ tensor represents longitudinal modes and the transverse modes are represented by $E_{x'}$ and A_1 tensors. According to Table I, only transverse modes are allowed in any of the four polarization configurations. Furthermore, it is important to note that only the A_1(TO) mode is allowed in $y'(z',z')\overline{y'}$ configuration whereas $E_{x'}$(TO) is the only allowed mode in $y'(z',x')\overline{y'}$ configuration. Hence, any difference in the TO phonon energy between the two polarization configurations is due to the ordering-induced anisotropy (A_1-E splitting) of the $GaInP_2$ crystal. Two Raman spectra with $y'(z',z')\overline{y'}$ and $y'(z',x')\overline{y'}$ are displayed in Fig. 1; the A_1(TO) phonon energy is observed at 330.1 cm^{-1}, $\sim 2.1\ \mathrm{cm}^{-1}$ higher than that of $E_{x'}$(TO). It is known that the bonds along the ordering axis gets stiffer as the order parameter increases.[10] Since A_1(TO) represents a vibration along the ordering axis and $E_{x'}$(TO) represents a vibration perpendicular to it, one would expect that the phonon frequency for A_1(TO) is higher than that for $E_{x'}$(TO). The distinct difference in the TO phonon energy between the two Raman spectra provides clear evidence of a small anisotropy induced by spontaneous

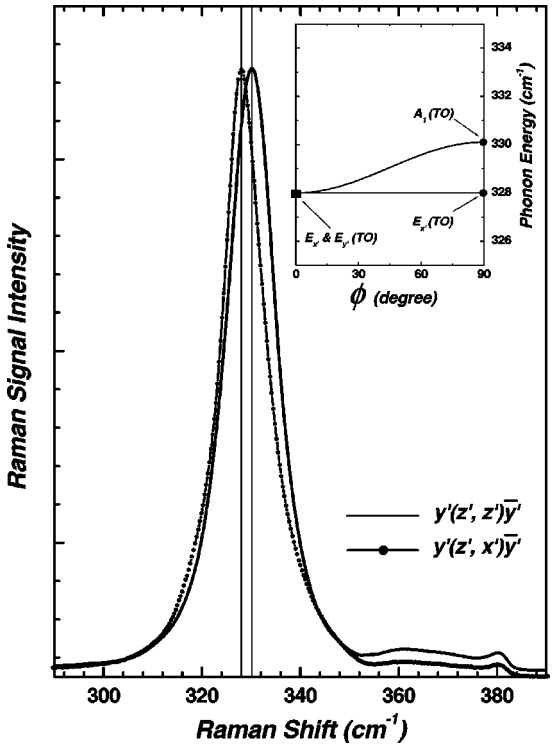

FIG. 1. Raman spectra measured in $y'(z',z')\overline{y'}$ (solid line) and $y'(z',x')\overline{y'}$ (dotted solid line) polarization configurations, excited with the 7352-Å line from a tunable Ti:sapphire laser. The $y'(z',x')\overline{y'}$ spectrum is enlarged by a factor of 4 to facilitate the comparison of the TO phonon signatures. Angular dispersion of the TO modes is illustrated in the inset, where the two circular dots indicate the TO modes experimentally observed at 328.0 cm^{-1} and 330.1 cm^{-1}, the error bars ($\sim$ 0.32 cm^{-1}) are slightly smaller than the size of these dots. The continuous angular variation is indicated with a simple guideline (Ref. 12) representing $\sqrt{330.1^2\sin^2\phi+328.0^2\cos^2\phi}$.

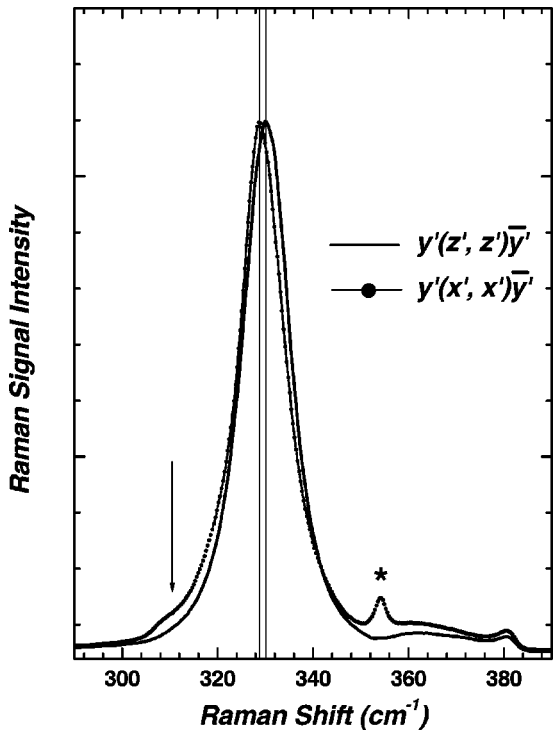

FIG. 2. Raman spectra measured in $y'(z',z')\bar{y}'$ (solid line) and $y'(x',x')\bar{y}'$ (dotted solid line) polarization configurations, excited with a Ti:sapphire laser tuned at 7352 Å. The $y'(z',z')\bar{y}'$ spectrum is enlarged by a factor of 2 to facilitate the comparison of the TO phonon signatures. The spectral uncertainty in the Raman shift is ~ 0.32 cm^{-1}.

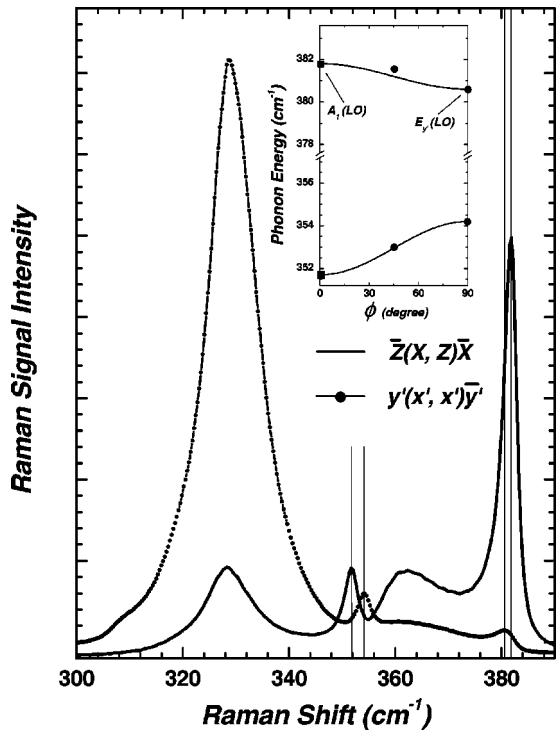

FIG. 3. Raman spectra measured in $y'(x',x')\bar{y}'$ (dotted solid line) and $\bar{Z}(X,Z)\bar{X}$ (solid line) scattering geometries, excited with a Ti:sapphire laser tuned at 7352 Å. Angular dispersions of the two phonon modes are illustrated in the inset, where circular and square dots represent the experimentally observed modes, using $\sqrt{380.6^2\sin^2\phi+381.8^2\cos^2\phi}$ for the upper curve and $\sqrt{354.2^2\sin^2\phi+351.7^2\cos^2\phi}$ for the lower one. The error bars (~ 0.32 cm^{-1}) are slightly smaller than the size of these dots.

ordering in the $GaInP_2$ crystal. It is interesting to notice that the A_1(TO) phonon signature observed in the $y'(z',z')\bar{y}'$ geometry is slightly broader than that for $E_{x'}$(TO) in $y'(z',x')\bar{y}'$ by ~ 1.5 cm^{-1}. As the angle ϕ between the phonon wave vector $\boldsymbol{q}$ and the ordering axis ($\boldsymbol{z}'$) changes from 0° to 90°, the A_1(TO) frequency shows a continuous variation from the degenerate value (328.0 cm^{-1}) to the maximally split value (330.1 cm^{-1}) while the $E_{x'}$(TO) mode does not exhibit any change, which is illustrated in the inset of Fig. 1. Due to the use of a 60× microscope objective, the phonon wave vector is not purely perpendicular to the ordering axis but contains a small contribution from ϕ less than 90° in our $y'(z',z')\bar{y}'$ Raman measurements, leading to the slightly broader Raman signature for $y'(z',z')\bar{y}'$ configuration.

In the $y'(x',x')\bar{y}'$ geometry, both A_1(TO) and $E_{x'}$(TO) are allowed with Raman efficiencies a^2 and c^2, respectively, making the TO phonon signature in this scattering geometry a superposition of the two TO modes. As shown in Fig. 2, the peak position of the TO phonon signature in $y'(x',x')\bar{y}'$ is observed at the Raman shift smaller than that in $y'(z',z')\bar{y}'$ by ~ 1.3 cm^{-1},[16] which is another confirmation of the anisotropy of the TO modes manifested in Fig. 1. Although LO phonon Raman scattering is forbidden in this (110) backscattering geometry, small signatures of the LO modes around ~ 360 cm^{-1} and ~ 380 cm^{-1} are observed and can be partly due to the geometry of the micro-Raman optics employed in this study as discussed earlier. However, there is a clear directionality; the forbidden modes are distinctly stronger for the $y'(x',x')\bar{y}'$ configuration than for the $y'(z',z')\bar{y}'$, and the so-called 354 cm^{-1} mode labeled with an asterisk exhibits a striking difference in its selection rule from the LO phonon signature around ~ 380 cm^{-1}. Since the excitation energy, ~ 1.69 eV, is not far from the fundamental band gap of the sample, ~ 1.80 eV, at room temperature this indicates that the Fröhlich interaction is involved, making these forbidden modes partially observable.[17] In addition to the forbidden LO phonon signatures, a shoulderlike feature identified with an arrow, which is absent in $y'(z',z')\bar{y}'$ configuration, is observed at ~ 310 cm^{-1} in the $y'(x',x')\bar{y}'$ configuration. A point group analysis for a crystal of C_{3v} symmetry yields nine Raman-active modes, i.e., $3A_1(z)+3\{E(x)+E(y)\}$, at the zone center of the perfectly CuPt-ordered $GaInP_2$. To the best of our knowledge, only seven Raman modes[18] have been experimentally identified although there have been some theoretical predictions regarding the *missing modes*.[19,20] Since these ''missing modes'' originate from the zone boundary TO phonon (L point) of a random $GaInP_2$ alloy and become Raman-active due to Brillouin zone folding induced by spontaneous ordering, one would expect that their frequency

should be slightly lower than that of the TO mode at $\sim 330\ \mathrm{cm}^{-1}$, which evolves from the zone center TO phonon (Γ-point) of a random $GaInP_2$ alloy.[19,20] Therefore, we identify the mode observed at $\sim 310\ \mathrm{cm}^{-1}$ in Fig. 2 with the ''missing modes'' represented by the $E_{x'}$ and $E_{y'}$ tensors.[21]

In order to probe phonons whose wave vector $\boldsymbol{q}$ are along the ordering axis we have employed a right-angle scattering geometry where the incident light is in the $\overline{Z}$ direction and the scattered in the $\overline{X}$ direction. For a sample grown on a 6° misoriented substrate, the angle between $\boldsymbol{z}'$ and $\boldsymbol{Z}$ is 48.7°. Therefore, in this geometry it is a good approximation to assume that $\boldsymbol{q}$ is parallel to $\boldsymbol{z}'$ and the A_1 tensor represents longitudinal modes and the $E_{x'}$ and $E_{y'}$ tensors transverse modes. The Raman spectrum measured in $\overline{Z}(X,Z)\overline{X}$ configuration, where both A_1 and $E_{x'}$ modes are allowed, is displayed and compared to that measured in the $y'(x',x')\overline{y'}$ configuration in Fig. 3. The anisotropy of the LO phonon mode at $\sim 380\ \mathrm{cm}^{-1}$ is clearly evidenced by its unmistakable $-1.2\ \mathrm{cm}^{-1}$ phonon frequency shift as it changes from a $A_1(\mathrm{LO})$ mode in the $\overline{Z}(X,Z)\overline{X}$ configuration to an $E_{y'}(\mathrm{LO})$ mode in the $y'(x',x')\overline{y'}$ configuration. The frequency change of the LO mode at $\sim 380\ \mathrm{cm}^{-1}$ can be understood in terms of stiffening of the bond along the ordering axis as discussed earlier in the case of TO mode at $\sim 330\ \mathrm{cm}^{-1}$. In surprising contrast, the phonon mode at $\sim 354\ \mathrm{cm}^{-1}$, whose origin can be traced to the folding of LO phonon dispersion, exhibits an even larger shift in the opposite direction, $+2.5\ \mathrm{cm}^{-1}$, as the angle ϕ between $\boldsymbol{q}$ and the ordering axis changes from 0° to 90°. The angular dispersions for the two phonon modes were further confirmed by measuring Raman spectrum in $X(y',y')\overline{X}$ scattering configuration where $\phi \approx 45°$ and the corresponding Raman frequencies are indicated with circular dots around $\phi \approx 45°$ in the inset of Fig. 3. It should be pointed out, however, that the currently available theoretical studies[19,20] do not provide satisfactory accounts for our experimental data on the anisotropy of the $\sim 354\ \mathrm{cm}^{-1}$ mode. It appears that further theoretical investigation is necessary in order to explain our experimental result for the angular dispersion of the vibrational mode at $\sim 354\ \mathrm{cm}^{-1}$.

In conclusion, we have studied the anisotropy associated with the angular variation of the phonon wave vector $\boldsymbol{q}$ with respect to the ordering axis $\boldsymbol{z}'$ of a spontaneously ordered $GaInP_2$ by carefully performing micro-Raman measurements in scattering geometries where $\boldsymbol{q}$ is either parallel or perpendicular to $\boldsymbol{z}'$. We found that the LO mode at $\sim 380\ \mathrm{cm}^{-1}$ and the TO mode at $\sim 330\ \mathrm{cm}^{-1}$ exhibit a distinct phonon frequency change of $-1.2\ \mathrm{cm}^{-1}$ and $+2.1\ \mathrm{cm}^{-1}$, respectively, as the angle ϕ between $\boldsymbol{q}$ and $\boldsymbol{z}'$ varies from 0° to 90°. This small angular dispersion is explained on the basis of the bond-stiffening along the ordering axis with increasing order parameter η, providing strong evidence for a small A_1-E splitting compared to a large LO-TO splitting for these modes. In addition, we observed an even larger angular dispersion, $+2.5\ \mathrm{cm}^{-1}$, for the phonon mode at $\sim 354\ \mathrm{cm}^{-1}$, giving strong motivation for further theoretical investigation. Finally, we experimentally identified two additional modes that have been labeled as *missing* in order to account for all nine Raman-active optical modes, i.e., $3A_1(z)+3\{E(x)+E(y)\}$.

We thank S. Smith for experimental assistance. This work was supported by the Office of Science (Material Science Division) of the Department of Energy under Contract No. DE-AC36-99GO10337.

[1] For a review of recent progress in this field, see G.B. Stringfellow, MRS Bull. **22(7)**, 27 (1997).
[2] T. Suzuki, A. Gomyo, S. Iijima, K. Kobayashi, S. Kawata, I. Hino, and T. Yuasa, Jpn. J. Appl. Phys., Part 1 **27**, 2098 (1988).
[3] M. Kondow and S. Minagawa, J. Appl. Phys. **64**, 793 (1988).
[4] K. Sinha, A. Mascarenhas, G.S. Horner, R.G. Alonso, K.A. Bertness, and J.M. Olson, Phys. Rev. B **48**, 17 591 (1993).
[5] K. Sinha, A. Mascarenhas, G.S. Horner, K.A. Bertness, S.R. Kurtz, and J.M. Olson, Phys. Rev. B **50**, 7509 (1994).
[6] K. Uchida, P.Y. Yu, N. Noto, Z. Liliental-Weber, and E.R. Weber, Philos. Mag. B **70**, 453 (1994).
[7] F. Alsina, N. Mestres, J. Pascual, C. Geng, P. Ernst, and F. Scholz, Phys. Rev. B **53**, 12 994 (1996).
[8] A.M. Mintairov and V.G. Melehin, Semicond. Sci. Technol. **11**, 904 (1996).
[9] A. Hassine, J. Sapriel, P. Le Berre, M.A. Di Forte-Poisson, F. Alexandre, and M. Quillec, Phys. Rev. B **54**, 2728 (1996).
[10] H.M. Cheong, A. Mascarenhas, P. Ernst, and C. Geng, Phys. Rev. B **56**, 1882 (1997).
[11] H.M. Cheong, F. Alsina, A. Mascarenhas, J.F. Geisz, and J.M. Olson, Phys. Rev. B **56**, 1888 (1997).
[12] W. Hayes and R. Loudon, *Scattering of Light by Crystals* (Wiley, New York, 1978).
[13] For sample growth and other experimental details, see Ref. 11.
[14] Due to the substrate misorientation, the growth direction is not exactly [001] but tilted by 6°. For simplicity, we denote the growth direction as $Z=[001]$ in this paper.
[15] This accuracy is obtained by carefully testing all possible source of errors including the instability of the laser, the spectrograph with a charge-coupled device (CCD), and the overall optical system itself with respect to drift (due to temperature fluctuation, etc.) over a period of 1 h.
[16] Excitation with 5145-Å line from an Ar^+ laser tends to increase this value up to $\sim 1.6\ \mathrm{cm}^{-1}$. This can be attributed to the fact that the 7352-Å excitation exhibits a stronger resonance effect and hence follows the Raman selection rule less faithfully than the 5145-Å excitation, producing slightly different contributions from $A_1(\mathrm{TO})$ and $E_{x'}(\mathrm{TO})$ modes for different excitation energies.
[17] H.M. Cheong, A. Mascarenhas, J.F. Geisz, and J.M. Olson, Phys. Rev. B **62**, 1536 (2000); Fig. 3 there clearly illustrates the resonance enhancement of the forbidden LO scattering as the exci-

tation energy approaches the band gap.

[18] The seven modes are the $E_{x',y'}$ mode at $\sim 60\ \mathrm{cm}^{-1}$, A_1 mode at $\sim 205\ \mathrm{cm}^{-1}$, $E_{x',y'}$ mode at $\sim 330\ \mathrm{cm}^{-1}$, A_1 mode at $\sim 354\ \mathrm{cm}^{-1}$, and A_1 mode at $\sim 380\ \mathrm{cm}^{-1}$.

[19] F. Alsina, H.M. Cheong, N. Mestres, J. Pascual, and A. Mascarenhas, in *Self-Organized Processes in Semiconductor Alloys*, edited by A. Mascarenhas, D. Follstaedt, T. Suzuki, and B. Joyce, MRS Symposia Proceedings No. 583 (Materials Research Society, Warrendale, 2000), p.223.

[20] V. Ozolins and A. Zunger, Phys. Rev. B **57**, R9404 (1998).

[21] Although we have clearly observed this mode in one of the right-angle scattering geometry, $\overline{Z}(Y,Y)\overline{X}$, a systematic selection rule analysis based on the C_{3v} Raman tensors would require further investigation to overcome the difficulty associated with very weak intensity of this mode and its spectral position near the strong TO mode at $\sim 330\ \mathrm{cm}^{-1}$ and will not be discussed further in this paper.